NASA Technical Memorandum 108827

Turbulence Compressibility Corrections

T. J. Coakley, C. C. Horstman, J. G. Marvin, J. R. Viegas, J. E. Bardina, P. G. Huang, and M. I. Kussoy, Ames Research Center, Moffett Field, California

May 1994

National Aeronautics and Space Administration

Ames Research Center
Moffett Field, California 94035-1000

Summary

The basic objective of this research was to identify, develop and recommend turbulence models which could be incorporated into CFD codes used in the design of the NASP vehicles. To accomplish this goal, a combined effort consisting of experimental and theoretical phases was undertaken. The experimental phase consisted of a literature survey to collect and assess a database of well documented experimental flows, with emphasis on high speed or hypersonic flows, which could be used to validate turbulence models. Since it was anticipated that this database would be incomplete and would need supplementing, additional experiments in the NASA Ames 3.5' hypersonic wind tunnel (HWT) were also undertaken. The theoretical phase consisted of identifying promising turbulence models through applications to simple flows, and then investigating more promising models in applications to complex flows. The complex flows were selected from the database developed in the first phase of the study. For these flows it was anticipated that model performance would not be entirely satisfactory so that model improvements or corrections would be required. The primary goals of the investigation were essentially achieved. A large database of flows was collected and assessed, a number of additional hypersonic experiments were conducted in the Ames HWT, and two turbulence models (k-ε and k-ω models with corrections) were determined which gave superior performances for most of the flows studied and are now recommended for NASP applications.

Introduction

With the advent of the hypersonic airplane, hypersonic flows are receiving special attention from researchers in computational fluid dynamics. Complex flow phenomena such as shock-wave boundary layer interactions, separation and combustion are of particular interest because of their importance to the successful design of structural, propulsive and thermal protection systems. Rapid advances in CFD in recent years have resulted in its increased use as a design tool for aeronautical systems and have lead to reductions in the time and costs of wind tunnel testing. A major obstacle to the use of CFD as a design tool is its dependence on turbulence modeling for accurate prediction of complex flows. Although recent advances have been made in turbulence modeling, many more will be required before CFD can be applied with confidence to a wide range of flow problems. This is especially true at hypersonic speeds where high temperatures and pressures

create additional difficulties for turbulence modeling and where wind tunnel experiments which can be used to validate models are sparse.

The overall goal of this research is to identify, develop and recommend turbulence models which can be incorporated into the CFD codes used in the design of the NASP vehicle. To accomplish this objective, a combined and joint effort consisting of experimental and theoretical phases was undertaken. The objective of the experimental phase was to conduct a literature survey to identify and assess a database of well documented experimental flows which could be used to validate turbulence models. Since it was anticipated that this database would be incomplete, it was also decided to perform additional experiments in the NASA Ames 3.5' hypersonic wind tunnel (HWT) to supplement the database.

The objective of the theoretical phase was to identify promising turbulence models through applications to simple flows, such as flat plate flows, and to then investigate the more promising models in applications to more complex flows. The complex flows were to be selected from the database developed in the first phase of the study. For these flows it was anticipated that model performance would not be entirely satisfactory so that model improvements or corrections would be required. The flows of interest were restricted to ideal gas flows because of the sparsity of high quality experimental validation data and viable turbulence models for real gas flows.

The schedule of tasks and milestones for the completion of the research on Government Work Package 18 is shown in fig. 1. With this report the work is essentially complete with the exception of the compressible shear layer experiment in the Ames 3.5' HWT. Completion of this experiment was halted due to the lack of funds caused by funding reductions in the NASP project.

The report is organized into 7 sections. Following the introduction, two sections on the experimental phase of the study will be presented including one on the database collection and assessment and another on the experiments conducted in the Ames 3.5' HWT. Next, sections describing the theoretical phase of the study will be presented. These include sections on recommended baseline turbulence models, compressibility corrections recommended for improved predictions of complex flows and representative results of numerical predictions using the baseline and corrected models. Finally, the report con-

cludes with a summary of basic results and recommendations including topics for future study.

Database Collection and Assessment

As stated in the introduction, the purpose of the database collection and assessment activity was to provide a base of reliable and well documented wind tunnel experiments by means of which turbulence models could be validated. These experiments, for the most part, involve relatively simple geometric shapes which may be viewed as separate elements of an overall vehicle. The results of this activity are reported by Settles and Dodson (1991, 1993a and 1993b) and will be summarized here.

Settles and Dodson (1991 and 1993b) provide a survey and assessment of experiments involving two and three dimensional shock-wave boundary-layer interaction flows. Eight hundred experiments were initially identified for further review. Of these, 112 distinct experiments were found involving flows at Mach 3 and above. The acceptance criteria applied to these included: 1) Measurements of surface pressures, skin friction and/or heat transfer, and velocity, temperature, or pitot pressure profiles at selected locations, 2) well defined experimental boundary conditions, 3) well defined error bounds, 4) adequate spatial resolution of measurements and 5) full documentation of tabulated data. For hypersonic conditions, i.e. $M > 5$, only 7 studies passed the acceptance criteria and only three were three dimensional. An additional 11 experiments passed the criteria at supersonic speeds.

The survey and assessment of attached boundary layer and free shear flow experiments is given by Settles and Dodson (1993a). The acceptance criteria applied to these cases was identical to that applied to the shock-wave boundary-layer interaction experiments. For the boundary layer experiments, 153 candidate cases were identified for further review. Of these 39 were subjected to the acceptance criteria. No hypersonic and only 9 supersonic cases passed. For the free shear layer experiments, 1137 candidate cases were identified for further review. Of these, 45 were subjected to the acceptance criteria and only 3 passed.

Experiments in the NASA Ames 3.5' Hypersonic Wind Tunnel

The experiments were conducted in the Ames 3.5' hypersonic wind tunnel and were done with relatively simple generic shapes such as cones, cylinders, plates and wedges. These shapes were chosen to typify locations on a high speed vehicle where turbulence modeling was expected to be a critical issue. The experiments were run at nominal Mach numbers ranging from 7 to 8.3 and unit Reynolds numbers (per meter) from 4.9 to 5.8 million. Boundary-layers approaching the interaction region were relatively large, with thicknesses on the order of 2.5 to 3.7 cm, which allowed detailed flow field surveys to be easily made. In most of the experiments, both surface measurements and flow field (profile) measurements were made including initial boundary conditions required to start numerical computations. With two minor exceptions, the experiments passed the acceptance criteria described in the previous section. In addition, an analysis of measurement errors was made and documented. The results of these experiments are described in detail by Kussoy et al (1989; 1991a,b; 1992; 1993a,b,c) and Horstman and Kussoy (1989) and the data have been made available on floppy disks.

M = 7 Hypersonic Cylinder-Flare and Fin flows

The test bed employed in this experiment consisted of an ogive-cylinder at zero angle of attack with a series of removable symmetric flares or sharp fins (see figs. (2a and 2b)). Both flare and fin angles were varied, producing shock waves of various strengths, and resulting in both attached and separated flow fields. Detailed measurements verified a fully developed turbulent boundary- layer on the cylinder ahead of the interaction region. The resulting flows were axisymmetric with and without separation for the flare case, and three dimensional with separation for the fin case. Surface pressures and heat transfer rates were measured on both configurations, and flow field surveys were done on the flare configuration. The results are reported in Kussoy and Horstman (1989) and Horstman and Kussoy (1989).

M = 8.2 2-D Wedge and 3-D Vertical Fin Flows

A flat plate arrangement was used for this experimental series and is shown in fig.(3). It was of a hollow modular construction, enabling both test bodies and instrumen-

tation to be easily manipulated and changed. The full length of the wind tunnel test section was utilized in the design and because of this a well developed equilibrium turbulent boundary-layer was present at the shock interaction zone. Two configurations were tested; the first consisted of a sharp wedge supported over the width of the test section, the second was a sharp vertical fin attached to the plate surface. These are both illustrated in fig.(3). Both the wedge and fin angles were varied, producing shock-wave boundary-layer interactions of varying strength with a maximum wall-pressure ratio of p/p_∞ = 21.5 and 6.4, respectively. This resulted in both attached and separated flow fields for the wedge flows, and swept three dimensional vortical flow fields for the fin flows. Detailed surveys verified a fully developed hypersonic turbulent boundary-layer on the flat plate ahead of the interaction zone.

For the wedge configuration, only surface conditions were measured. For the fin configuration, however, mean flow profile surveys were also taken - both in the undisturbed and interaction regions - and from them pitot pressure contours and boundary-layer thickness parameters were obtained. We believe this is the first fully three dimensional shock-wave boundary-layer interaction flow to be so documented at hypersonic speeds. Results for both configurations are reported in Kussoy et al (1991a,b;1992). Experimental and computational results for the 10° and 15° vertical fin flows are discussed in the section on Model Validation-Representative Results.

M = 8.3 Crossing Shock Flow

For the third series of experiments, a configuration was chosen to reflect several key elements of a generic hypersonic inlet. These included a thick turbulent boundary-layer approaching two vertical fins of varying wedge angle, a crossing shock pattern produced by the fins, boundary-layer vortices, large pressure gradients, and separation zones. The test body for this series of experiments is shown in fig.(4).

Streamwise and transverse surface pressure and heat transfer distributions were measured as well as flow field surveys of pitot pressure and flow angle. One important result of these measurements should be mentioned here. This was the persistence of an extensive low pressure region far downstream of the fin leading edges. This low pressure region implied that the generic inlet tested here would not be a very efficient pressure diffusing device. The experimental results for this configuration are given in Kussoy et al

(1993a,b,c). experimental and computational results for the 15° fin-angle case are discussed in the section on Model Validation-Representative Results.

Recommended Baseline Turbulence Models

The baseline turbulence models recommended for use in NASP applications will be described in this section. A variety of turbulence models have been investigated in varying degrees throughout the course of the study. They include 0-eq, 1-eq, and 2-eq eddy viscosity models, and Reynolds stress transport models. For NASP applications, the primary emphasis has been placed on 2-eq models and these models will be the only ones described in detail here. Descriptions of other models used in the course of the study, and results obtained with them, are given in Coakley and Huang (1992) and Coakley and Marvin (1993), Horstman (1991,1992), and Huang and Coakley (1993a,b).

The models investigated and recommended here are those that utilize no slip boundary conditions at solid walls and involve the use of wall damping functions (in most cases). This is in contrast to conventional practice with two equation models in which wall functions and essentially slip type boundary conditions are used. This choice was made because at the very high speeds of hypersonic flight, the effective Reynolds numbers of the flows can be quite low, in some cases involving transition and relaminarization. In these cases, the thickness of the laminar sublayer becomes an appreciable fraction of the overall boundary layer thickness and the wall function approach becomes inapplicable or ineffective. In addition, the wall function approach gives questionable results for separated flows. For these reasons it was decided to use the wall damping function approach.

Two equation models have been emphasized since these are viewed as the simplest and most practical models available which have sufficient generality to be applied to the complex flows of interest in NASP applications. Although numerous two equation models have been investigated, descriptions of only two of these will be given here since these are the baseline models of our final recommendation. In Coakley and Huang (1992) a detailed investigation of the performance of a variety two equation models was presented for flat plate boundary layers over a wide range of Mach and Reynolds numbers. The results of that study showed that most of the models gave reasonably good predictions of skin friction, heat transfer and velocity profiles with little clear preference of one model over the other. For this reason only two models were selected for further study, and it is

believed that these models are representative of most two equation models currently in use. The baseline models are the k-ε model of Jones and Launder (1972), as modified by Launder and Sharma (1973), and the k-ω model of Wilcox (1984). These models are used with the (mass weighted) Reynolds averaged compressible Navier-Stokes equations which, in cartesian tensor form, are given below.

Reynolds Averaged Compressible Navier-Stokes Equations

$$\frac{\partial}{\partial t}(\rho) + \frac{\partial}{\partial x_j}(\rho u_j) = 0$$

$$\frac{\partial}{\partial t}(\rho u_i) + \frac{\partial}{\partial x_j}(\rho u_i u_j + \sigma_{ij}) = 0$$

$$\frac{\partial}{\partial t}(\rho E) + \frac{\partial}{\partial x_j}(\rho E u_j + u_i \sigma_{ij} + q_j) = 0$$

where; ρ is the density; u_i are the cartesian velocity components; $E = e + 0.5u_iu_i + k$ is the total specific energy; $e = c_vT$ is the specific internal energy; $k = 0.5\ \overline{\rho u_i'' u_i''} / \overline{\rho}$ is the turbulent kinetic energy; T is the temperature; $p = (\gamma - 1)\rho e$ is the equation of state; and p is the pressure; $\gamma = c_p/c_v$ is the ratio of specific heats, and c_p and c_v are the specific heats at constant pressure and volume respectively. The variables σ_{ij} and q_j are the total stress tensor and heat flux vector, respectively, which include both molecular and (Reynolds averaged) turbulent contributions. Using the Boussinesq approximation, these variables are represented in terms of an eddy viscosity by

$$\sigma_{ij} = \delta_{ij}\left(p + \frac{2}{3}\rho k\right) - (\mu + \mu_T)\left(\frac{\partial u_i}{\partial x_j} + \frac{\partial u_j}{\partial x_i} - \frac{2}{3}\delta_{ij}\frac{\partial u_k}{\partial x_k}\right)$$

$$q_j = -\gamma\left(\frac{\mu}{\sigma} + \frac{\mu_T}{\sigma_T}\right)c_v\frac{\partial T}{\partial x_j} - \left(\mu + \frac{\mu_T}{\sigma_k}\right)\frac{\partial k}{\partial x_j}$$

where μ and μ_T are the molecular and turbulent (eddy) viscosities σ and σ_T are molecular and turbulent Prandtl numbers with $\sigma = c_p\mu/\kappa$ (assuming air) $\sigma_T = 0.9$ and σ_k depending on the model used. The turbulent eddy viscosity is expressed in terms of the turbulent kinetic energy, k, and either the dissipation rate, ε, or the specific dissipation rate ω

depending on the model. This expression is

$$\mu_T = C_\mu f_\mu \rho \sqrt{k} l = C_\mu f_\mu \rho \frac{k^2}{\varepsilon} = C_\mu f_\mu \rho \frac{k}{\omega} \qquad , \qquad \omega = \frac{\varepsilon}{k}$$

where $\sqrt{k}$ is the turbulent velocity scale, $l = \sqrt{k^3}/\varepsilon = \sqrt{k}/\omega$ is the length scale, C_μ is a modeling constant, and f_μ is a damping function depending on the specific model used. For applications to complex flows, the governing equations were expressed in terms of curvilinear coordinates and solved using the finite volume method, Viegas and Rubesin (1991), and Huang and Coakley (1992b) or the finite difference method, Bardina (1994).

The recommended baseline k-ε and k-ω turbulence models are expressed by the formulas given below.

$$\frac{\partial}{\partial t}(\rho k) + \frac{\partial}{\partial x_j}(\rho k u_j - \mu_k \frac{\partial k}{\partial x_j}) = (P_k (\frac{S}{\omega})^2 - \frac{2}{3}\frac{D}{\omega} - D_k)\rho\omega k$$

$$\frac{\partial}{\partial t}(\rho s) + \frac{\partial}{\partial x_j}(\rho s u_j - \mu_s \frac{\partial s}{\partial x_j}) = (P_s (\frac{S}{\omega})^2 - \alpha_s \frac{D}{\omega} - D_s)\rho\omega s$$

$$S = \left(\frac{\partial u_i}{\partial x_j} + \frac{\partial u_j}{\partial x_i}\right)\frac{\partial u_i}{\partial x_j} - \frac{2}{3}\left(\frac{\partial u_k}{\partial x_k}\right)^2 \qquad , \qquad D = \frac{\partial u_k}{\partial x_k}$$

In these equations and in the following Tables, variable "s" and subscript "s" are replaced with ε for the k-ε model or ω for the k-ω model, respectively.

The model parameters are defined in Tables 1, 2 and 3

Table 1: Model Parameters

$C_\mu = 9/100$	$\mu_k = \mu + \mu_T/\sigma_k$	$\mu_s = \mu + \mu_T/\sigma_s$
$R_T = k^2/\nu\varepsilon = k/\nu\omega$	$P_k = C_\mu f_\mu$	$P_s = C_{sl} P_k$
$\alpha_s = 2/3\ C_{sl}$	$\nu = \mu/\rho$	$\nu_T = \mu_T/\rho$

Table 2: Launder-Sharma k-ε Model, $s \equiv \varepsilon = \omega k$

$\sigma_k = 1$	$\sigma_\varepsilon = 1.3$
$C_{\varepsilon 1} = 1.45$	$C_{\varepsilon 2} = 1.92$
$f_\mu = \exp(-3.4/(1.0 + R_T^2/50))$	$f_2 = 1 - 0.3 \exp(-R_T^2)$
$D_k = 1 + (2\nu/\varepsilon)\,(\partial k^{1/2}/\partial x_k)^2$	$D_\varepsilon = C_{\varepsilon 2} f_2 - (2\nu\,\nu_T/\varepsilon^2)\,(\partial^2 (u_k u_k)^{1/2}/\partial x_k \partial x_k)^2$

Table 3: Wilcox k-ω Model, $s \equiv \omega = \varepsilon/k$

$\sigma_k = 1/2$	$\sigma_\omega = 1/2$	$C_{\omega 1} = 5/9$	$C_{\omega 2} = 5/6$	$f_\mu = 1$	$D_k = 1$	$D_\omega = C_{\omega 2}$

For the Launder-Sharma model, the thin layer approximation was normally used to compute the derivatives in the D_k and D_ε terms.

An important consideration in using the Wilcox k-ω model, which is not necessary with the k-ε model, is the value of ω in the free stream (just outside the boundary-layer edge) where it cannot be too small. In all of the applications of this study, it was possible to choose values of ω at the inflow boundary which insured that the values of ω in the free stream would not be too small. (It must be chosen such that $\omega_\infty > 10\, U_\infty/L$ where U_∞ is the free stream velocity and L is the length of run of the boundary layer and ω_∞ is the free stream value of ω at the start of the boundary layer). It may be that in future applications it will not be feasable to control the free stream ω_∞ in this manner, and other measures will be necessary. One alternative would be to use the k-ω model of F. Menter (1992), which uses a blending of the k-ω and k-ε models to circumvent the problem. This model will be discussed more fully in the next section.

Recommended Model Corrections for Complex Flows

The baseline models described above are generally not adequate to accurately predict complex flow problems and must be corrected to deal with these cases. The types of modeling corrections that have been found useful in practice and which are recommended for NASP applications are summarized below. Other model corrections which have been tried in the course of the study but which are not recommended for applications are described in Coakley and Huang (1992).

Length Scale Correction

The first correction is addressed to difficulties encountered in predicting heat transfer in the reattachment or shock impingement zone of shock-wave boundary-layer interaction flows. In these zones, all 2-eq models dramatically overpredict heat transfer and must be corrected. The correction involves the use of an algebraic length scale which limits the slope of the length scale predicted by the two equation model, which otherwise would become very large in these regions. The formulas defining the length scale correction for the k-ε and k-ω models are given below,

$$l = min\{2.5y, \sqrt{k^3}/\varepsilon\} = min\{2.5y, \sqrt{k}/\omega\}$$

in these formulas, l is the turbulent length scale which is taken to be the smaller of an algebraic expression ($\kappa C_\mu^{-3/4}\, y = 2.5\, y$, based on a von Karman constant of $\kappa = 0.41$) and the conventional length scale given by the two equation model. Having computed this parameter, the value of ε or ω is recomputed and reset to be consistent with this value, e.g. $\varepsilon = \sqrt{k^3}/l$ or $\omega = \sqrt{k}/l$.

Rapid Compression Correction

The second correction to be described is called the rapid compression correction and is used to improve predictions of separation in shock-wave turbulent boundary-layer interactions. The correction involves changing the coefficient of the dilitation or velocity divergence in the ε and ω equations, i.e. α_ε or α_ω. The net effect of this correction is to increase the production of epsilon or omega in regions of rapid compression, or shock in waves, which reduces the eddy viscosity and enhances separation. The corrected values of the dilitation coefficient for each model are

$$\alpha_\varepsilon = 2 \qquad or \qquad \alpha_\omega = 4/3$$

as opposed to the Launder-Sharma coefficient $\alpha_\varepsilon = (2/3)\, C_{\varepsilon 1} = 0.97$ and the Wilcox coefficient $\alpha_\omega = (2/3)\, C_{\omega 1} = 0.37$ shown in Tables 1, 2, and 3. The development of this correction is discussed more fully in Coakley and Huang (1992).

Compressible Dissipation Correction

The third and final correction recommended for NASP applications is applicable to free shear flows (e.g. mixing layers, wakes and jets). In these types of flows, it is well known that shear layer spreading rates decrease as Mach numbers increase compared with spreading rates at zero Mach number. The correction recommended to improve predictions of these flows was developed originally by Zeman (1990), and is closely related to similar corrections developed by Sarkar (1991), and Wilcox (1992). The correction is listed below,

$$D_k \rightarrow D_k + \phi_k$$

$$D_\omega \rightarrow D_\omega - \phi_k$$

$$\phi_k = a_0 \left(1 - exp\left(-\left(max\left(0, a_1 M_T - a_2\right)/a_3\right)^2\right)\right)$$

D_ε is unchanged, $M_T = \sqrt{k}/c$, c is the local sound speed, $a_0 = 3/4$, $a_1 = \sqrt{(\gamma+1)}$, $a_2 = 1/10$, and $a_3 = 6/10$.

For applications involving boundary layers, or solid walls, this correction has been found to underpredict skin friction especially at high free stream Mach numbers. It is recommended, therefore, that this correction only be used in free shear flow applications. The correction of Wilcox (1992), which is similar to that of Zeman, has been found to work well in boundary layers as well as free shear flows and Wilcox recommends its use without reservation. Since we have not investigated this model under the wide range of conditions investigated using other model corrections, we chose not to recommend the model at this time.

Other Corrections and Models of Interest

Although the above models and corrections constitute our final recommendations for NASP applications, it is important to note that these models only constitute an improvement over previous models and may very well give poor predictions for flow situations which have not yet been investigated and validated. In this regard we draw attention to the k-ω model of F. Menter (1993), which has proven quite successful in incompressible and transonic flow applications. This model was designed to overcome certain defi-

ciencies of the Wilcox k-ω model and has certain features which might prove useful in hypersonic applications. One feature of the model is the so called shear stress transport or rapid strain feature which enables the model to give improved predictions of adverse pressure gradient boundary-layers and separation. This feature is similar to the rapid compression correction discussed above and enhances separation by reducing the eddy viscosity in non-equilibrium regions where the flow is changing rapidly. This feature was also tried with the baseline models and gave results very similar to those obtained with the rapid compression correction. It is believed that some combination of the two corrections may ultimately prove more accurate and reliable in future applications. It must be stated, however, that we did apply Menter's model to most of the flows described in this study and obtained no improvement over the recommended models. In some cases it did not perform as well. Since the model is considerably more complicated than the other models studied we decided not to include it in the list of recommended models.

Model Validation - Representative Results

Representative results of calculations and comparisons of model predictions with experimental measurements will be given in this section. The flows discussed include free shear (mixing layer) flows, 3 two dimensional shock-wave boundary- layer interaction flows, and 2 three dimensional shock-wave boundary-layer interactions. The turbulence models used include the recommended baseline and corrected k-ε and k-ω models.

Compressible Mixing layer

The first series of flows to be discussed consists of high speed mixing layers which are of considerable importance in the design of propulsive exhaust nozzles for the NASP vehicle. The comparisons of computations with experimental measurements is shown in fig.(5). The figure shows predictions of spreading rate divided by spreading rate at zero Mach number compared with experimental measurements over a range of convective Mach numbers. The data include the Bogdanoff (1993) compilation of the Langley data, and the measurements of Samimy and Elliot (1990). The calculations were done by Viegas and Rubesin (1992), who used the baseline k-ε model with the compressible dissipation corrections of Zeman and Sarkar. Although not shown, results obtained with the k-ω model give similar results. Examination of the comparisons indicates that the baseline model significantly overpredicts the spreading rate while the model corrections improve

the predictions. Of the two model corrections, the Zeman correction gives the best overall result.

Two-Dimensional Shock-Wave Boundary-Layer Interaction Flows

The second series of model validation studies to be discussed consists of two dimensional (planar and axisymmetric) shock-wave boundary-layer interactions. The flows are the Mach 7 ogive-cylinder-flare flow of Kussoy and Horstman (1989) (35° flare angle), the Mach 9 planar compression ramp flow of Coleman and Stollery (1972) (34° ramp angle), and the Mach 7 axisymmetric impinging shock flow of Kussoy and Horstman (1975) (15° generator angle). In all cases, the walls were highly cooled with wall-to-adiabatic wall temperature ratios on the order of 0.3 to 0.4. The test configurations for these cases are shown in figs.(6a,b,c).

All calculations were done using the code developed by Huang and Coakley (1992). The inlet flow conditions just ahead of the shock interaction zones were obtained by calculating the flow over a flat plate and matching measured and computed displacement thicknesses. The value of y^+ at the first grid point off the wall was maintained to be less than 0.5 and the grid was expanded exponentially from the wall to the free stream. This gave between 60 to 80 grid cells in the boundary-layer and 140 cells overall in the cross stream direction. Computations with fewer cells inside the boundary-layer (i.e. 40 cells) were made and no significant differences were observed. In the streamwise direction a grid of 140 cells was used except in the impinging shock case where 200 cells were used. The comparisons of computations with measurements are shown in figs.(7-9). They include measured and computed surface pressures and heat transfer distributions (and skin friction for the impinging shock case) and were done with the baseline and corrected k-ε and k-ω models. The pressure and heat transfer measurements are normalized by the measured values in the region ahead of the interaction. Zeman's compressible dissipation correction designed for shear layers was not used as explained in the section on model corrections. It is clear from these results that the baseline models significantly under predict the extent of separation and over predict the heat transfer in the interaction region. The corrected models both give results in much better agreement with experiment.

Three-Dimensional Shock-Wave Boundary-Layer Interaction flows

The Ames experiments on 3-D shock-wave boundary-layer interactions described in this report were used here to test the compressible turbulence models and the model corrections. The experiments and the data are also described in Settles and Dodson [1993a and 1993b] and Kussoy and Horstman [1991,1992,1993]. The calculations were done with the code of Bardina (1994)

3-D Vertical Fin Shock Interaction Flows

This experiment investigates the interaction of a hypersonic shock wave with a thick turbulent boundary layer [Kussoy and Horstman, 1991 and 1993b]. A 10° and a 15° vertical fins mounted on top of a flat plate were used to generate oblique shock waves. The free-stream Mach number was $M_\infty = 8.2$, the temperature was $T_\infty = 81°$ K, and the Reynolds number was $Re_\infty = 5 \cdot 10^6$ per meter. The wall temperature was fixed at 300° K. The interaction of the shock wave with the turbulent boundary layer generates a crossflow vortex separation with a "quasi conical" shape [Settles and Lu, 1985; Knight, Horstman, and Monson, 1992]. Peak wall pressure, skin friction, and heat transfer rates were observed in the re-attachment zone behind the crossflow vortex.

The numerical computations were made with 61x41x61 an 31x21x31 meshes [Bardina, Coakley, and Marvin, 1992]. Only small differences between the solutions were observed, and the fine mesh solutions are considered accurate for engineering purposes. The inflow conditions were obtained from the Navier-Stokes code solution matching the experimental displacement thickness.

A few comparisons of experiment and simulation with the finer mesh are described below. Figures 10a and 10b show the surface pressure and skin friction distributions, respectively, for the 10° fin flow on the flat plate surface at the crossed section located at x=0.1819 m downstream of the fin leading edge. Figure 10c shows the comparison of the wall heat transfer distribution on the flat surface at x=0.1645 m downstream of the fin leading edge. Comparable results for the 15° fin case are shown in fig.(11a,b,c). The symbols in the figures show the experimental data points, the solid lines show the solution with the baseline k-ω model, and the dash lines show the solution with the k-ω model with both model corrections (length-scale and rapid compression corrections). Both

simulations show good agreement with the experimental data. The peak values observed in the re-attachment zone are also well predicted. The simulations fail to predict the small plateau observed in the wall heat transfer rate distributions upstream of the shock wave. Comparison of baseline and corrected model predictions show only small differences. This is probably due to the fact that, compared with the 2-D results, the pressure rise through the shock wave is relatively weak and separation is relieved by three dimensional effects.

3-D Crossing Shock Interaction Flow

This experiment studies the interactions of two intersecting hypersonic shock waves with a thick turbulent boundary layer [Kussoy and Horstman, 1992]. Two 15° fins mounted on top of a flat plate were used to generate intersecting oblique shock waves (see fig. 4). The free-stream Mach number was $M_\infty = 8.3$, the temperature was $T_\infty = 80°$ K, and the Reynolds number was $Re_\infty = 5.3 \cdot 10^6$ per meter. The wall temperature was fixed at 300° K. The intersection of both crossflow vortices generates different complex flow structures with high static pressures and surface heat transfer rates. The intersection of the two "quasi conical" vortical structures uplifts the flow and induces a wave structure in the symmetry plane [Gaitonde and Shang, 1993].

The numerical simulations were made with a 231x81x81 mesh [Bardina and Coakley, 1994; Bardina, 1994]. Simulations studies with 101x61x41 and 31x21x31 grid points were also done to analyze grid effects. Small differences between the solutions were observed in the surface pressure and heat transfer distributions, but signifficant differences were observed in flow structure. The fine mesh solutions provided the best resolution of the turbulence structures and are considered accurate for engineering purposes. The inflow conditions were obtained from the Navier-Stokes code solution matching the experimental displacement thickness.

Figures 12a and 12b show the pressure and heat transfer distributions, respectively, on the plate surface along the symmetry plane located between the two fins. The symbols show the experimental data, the solid lines show the solution with the baseline k-ω model, and the dash lines show the solution with the k-ω model with both model corrections (length-scale and rapid compression corrections). Predictions of both surface pressure and heat transfer show good agreement, within the experimental uncertainty, except

near the outflow zone. The small plateau at the beginning of the interaction is also not predicted by either model. The peak pressure and heat transfer rate are very well predicted. As in the single fin cases, both the baseline and corrected model predictions show only small differences.

Figures 13a and 13b show the pressure distributions on the plate surface at two cross-sections, one located at $x/\delta_\infty = 5.60$ and the other located at $x/\delta_\infty = 6.92$ downstream of the fin leading edge. The first distribution is upstream of the peak surface pressure, and the second distribution is downstream of the peak surface pressure generated by the flow re-attachment. Both simulations show good agreement within the experimental uncertainty of the data, and both models give similar predictions.

Figures 13c and 13d show the comparison of heat transfer rate profiles on the plate surface in the crossed sections located at $x/\delta_\infty = 5.08$ and $x/\delta_\infty = 6.40$, respectively, upstream and downstream of the peak heat transfer rate observed in the symmetry plane. Both simulations agree in general with the experimental data. The model corrections show improved heat transfer rate predictions in the downstream zone.

Figure 14 shows experimental pitot pressure contours compared with computational contours obtained with the corrected k-ω model. Three locations are shown, x/δ_∞ = 5.60, 6.9, and 8.3, respectively. The resolution of the numerical data is 81x81 grid points while the resolution of the experimental data is 5x24, 4x24, and 4x24 respectively. The agreement with the experimental data is very good.

Summary and Conclusions

In this section we summarize the work performed under GWP 18, give our principal results and recommendations, and discuss plans for future work. We feel that, overall, the results produced in the course of the work were of a very high caliber and will be of considerable use to modelers and designers of hypersonic flight vehicles. The research was divided into two distinct phases; one experimental and the other theoretical. The experimental phase consisted of the collection and assessment of a database of high speed wind tunnel experiments gathered from sources around the world and the conduct of additional experiments in the NASA Ames 3.5' hypersonic wind tunnel which would add to the database. The primary aim of this effort was to produce a database of reliable and rele-

vant flow measurements which could be used to validate turbulence models for NASP CFD design codes. Out of a total of over 2000 experiments that were initially studied, the list of acceptable experiments was reduced a total of 30 using a set of strict acceptance criteria. The kinds of flows analyzed and recommended as legitimate candidates for inclusion in the database included two- and three-dimensional shock-wave boundary-layer interaction flows, attached boundary layers flows and free shear flows.

The theoretical phase of the work consisted of identifying, testing, and recommending turbulence models which would be of practical use in the CFD design codes. A large number of baseline models were initially tested on flat plate flows and this number was then reduced to two for further testing on more complex flows. The baseline models selected were the Launder-Sharma version of the k-ε model, and the Wilcox k-ω model. These models were tested on free shear flows and two- and three-dimensional shock-wave boundary-layer interaction flows. Some of the results of these calculations have been discussed in this report. It was found that the baseline models did not perform satisfactorily with regard to separation and heat transfer predictions especially for the 2-D shock-wave boundary-layer interaction flows, and did not accurately predict the spreading rate of free shear layers. To improve model performance for these complex flows, a series of compressibility corrections was investigated. The more promising of these corrections were then selected to be the final model recommendations for incorporation in to the NASP CFD codes. Representative results using the corrected models were discussed in this report. It was shown that for the flows investigated, the model corrections give substantially improved predictions.

Although the work performed in the course of this research has led to the identification of useful flows for model validation and the development of improved turbulence models for hypersonic flight, much work remains to be done. Not all of the flows included in the database of recommended flows have been investigated computationally, and these need to be investigated. More complicated flows not included in the database also need to be investigated. Flows that fall into this latter category include flows with chemical reactions such as those occurring in SCRAM jet combustion and propulsion, and flows that include transitional phenomena just to mention two. Interest in these and other areas of turbulence modeling research is very high and the work goes on.

References

Bardina, J. E. (1992), "Two-Equation Turbulence Modeling for Hypersonic Flight," NCC 2-585, NASA-CR-190313, NASA Ames Research Center, PR-92-010, MCAT Inst., CA.

Bardina, J., Coakley T., and Marvin, J. (1992), "Two-Equation Turbulence Modeling for 3-D Hypersonic Flows," AIAA Paper 92-5064, 4th International Aerospace Planes Conference, Orlando, FL.

Bardina, J. E. (1993), "Two-Equation Turbulence Modeling for Hypersonic Flight," NCC 2-585, NASA Ames Research Center, PR-93-07, MCAT Inst., CA, Feb.

Bardina, J. E., and Coakley, T. J. (1994), "Three-Dimensional Navier-Stokes Simulation with Two-Equation Turbulence Models of Intersecting Shock-Waves/Turbulent Boundary Layer at Mach 8.3," AIAA Paper 94-1905, Colorado Springs, CO.

Bardina, J. E. (1994), "Three-Dimensional Navier-Stokes Method with Two-Equation Turbulence Models for Efficient Numerical Simulation of Hypersonic Flows," AIAA Paper 94-2950, Indianapolis, IN.

Bogdanoff, D.W. (1983), "Compressibility Effects in Turbulent Shear Layers," *AIAA J.*, Vol. 21, No. 6, pp. 926-927.

Coakley, T. J., and Marvin, J. G. (1986), "Numerical Implementation and Performance of Turbulence Models for Compressible Flow Simulations," paper presented at First World Congress on Computational Mechanics, University of Texas, Arlington, TX.

Coakley, T. J., and Huang, P. G. (1990), "Evaluation of Turbulence Models for Hypersonic Flows," 8th National Aero-Space Plane Technology Symposium, Paper No. 24, Monterey, CA.

Coakley, T. J., Viegas, J. R., Huang, P. G., and Rubesin, M. W. (1990), "An assessment and Application of Turbulence Models for Hypersonic Flows," 9th National Aero-Space Plane Technology Symposium, Paper No. 106, Orlando, FL.

Coakley, T. J., and Huang, P. G. (1991), "Modeling for Compressible High Speed Flows," Tenth National Aero-Space Plane Technology Symposium, Paper No. 210, Monterey, CA.

Coakley, T. J., and Huang, P. G. (1992), "Turbulence Modeling for High Speed Flows," AIAA Paper 92-04366, Reno, NV.

Coakley, T. J., and Marvin, J. G. (1993), "Compressibility connections for Hypersonic Flow Turbulence Modeling," 1993 National Aero -Space Plane Technology Review, Monterey, CA.

Coakley, T. J., Huang, P. G., Bardina, J. E., and Viegas, J. R. (1993), "Modeling of Turbulence for Complex High Speed Flows," paper presented at Second National Congress on Computational Mechanics, Washington, D. C.

Coleman, G.T., and Stollery, J.L. (1972), "Heat Transfer from Hypersonic Turbulent Flow at a Wedge Compression Corner," *J. of Fluid Mech.*, Vol. 56, pp. 741-752.

Horstman, C. C., and Kussoy, M. I. (1989), "2- and 3-Dimensional Hypersonic Shock-Wave Turbulent-Boundary Layer Interaction Flows - Experiment and Computation," 6th NASP Symp., Monterey, CA.

Horstman, C. C. (1990), "Turbulence Modeling for Sharp-Fin-Induced Shock Wave/Turbulent Boundary-Layer Interactions," IUTAM Symp. on Separated Flows and Jets, Novosibirisk, USSR, Jul. 1990; also NASA TM 102828.

Horstman, C. C. (1991), "Hypersonic Shock-Wave Turbulent-Boundary-Layer Interaction Flows: Experiment and Computation (U)," 10th NASP Symp., Monterey, CA.

Horstman, C. C., Settles, G. S., and Dodson, L. J. (1991), "Hypersonic Shock-Wave Turbulent-Boundary-Layer Interaction Flows: Experiment and Computation," 10th NASP Symp., Monterey, CA.

Horstman, C. C. (1992), "Hypersonic Shock-Wave Turbulent-Boundary-Layer Interaction Flows," *AIAA J.*, Vol. 30, No. 6, pp. 1480-1481; also in AIAA Paper 91-1760, Honolulu, HI.

Huang, P. G., Bradshaw, P., and Coakley, T. J. (1992), "Assessment of Closure Coefficients for Compressible Flow Turbulence Models," NASA TM-103882.

Huang, P. G., and Coakley, T. J. (1992), "An Implicit Navier-Stokes Code for Turbulence Flow Modeling," AIAA Paper 92-0547, Reno, NV.

Huang, P. G., and Coakley, T. J. (1993), "Modeling Hypersonic Boundary-layer Flows with Second-moment Closure," present at the International Conference on Near Wall Turbulent Flows, Tempe, AZ.

Huang, P. G., and Coakley, T. J. (1993), "Calculations of Supersonic and Hypersonic Flows Using Compressible Wall Functions," presented at the 2nd International Symposium on Engineering Turbulence Modeling and Measurements, Florence, Italy.

Huang, P. G., and Coakley, T. J. (1993), "Turbulence Modeling for Complex Hypersonic Flows," AIAA Paper 93-0200, Reno, NV.

Huang, P. G., Bradshaw, P., and Coakley, T. J. (1993), "Skin Friction and Velocity Profile Family for Compressible Turbulent Boundary Layers," *AIAA J.*, Vol. 31, No. 9, pp. 1600 - 1604.

Huang, P. G., Bradshaw, P., and Coakley, T. J. (1994), "Turbulence Models for Compressible Boundary Layers", *AIAA J.*, Vol. 32, No. 4, pp. 735-740.

Huang, P. G., and Coleman, G.N. (1994), "On the van Driest Transformation and Compressible Wall-Bounded Flows", to be published in the *AIAA J.*

Kim, K.-S., Lee, Y., Alvi, F. S., Settles, G. S., and Horstman, C. C. (1991, "Skin Friction Measurements and Computational Comparison of Swept Shock/Boundary-Layer Interactions," *AIAA J.*, Vol. 29, No. 10, pp. 1643-1650.

Knight, D. D., Narayanswami, N., and Horstman, C.C. (1991), "A Numerical Investigation of the Interaction Between Crossing Oblique Shocks and a Turbulent Boundary Layer in Hypersonic Flow," 44th APS Annual Meeting, Tempe, AZ.

Knight, D. D., Settles, G. S., and Horstman, C. C. (1991), "Three-Dimensional Shock Wave Turbulent Boundary Layer Interactions Generated by a Sharp Fin at Mach 4," AIAA Paper 91.-0648, Reno, NV.

Knight, D. D., Horstman, C. C., and Monson, D. J. (1992), "The Hypersonic Shock Wave-Turbulent Boundary Layer Interaction Generated by a Sharp Fin at Mach 8.2," AIAA Paper 92-0747, Reno, NV.

Knight, D. D., Badekas, D., Horstman, C. C., and Settles, G. S. (1992), "On the Quasi-conical Flowfield Structure of the 3-D Single Fin Interaction," *AIAA J.*, Vol. 30, No. 12, pp. 2809-2816.

Knight, D. D., Horstman, C. C., and Bogdonoff, S. (1992), "Structure of a Supersonic Turbulent Flow Past a Swept Compression Corner," *AIAA J.*, Vol. 30, No. 4, pp. 890-896.

Kussoy, M. I., and Horstman, C. C. (1975), "An Experimental Documentation of a Hypersonic Shock-Wave Turbulent Boundary Layer Interaction Flow - with and without Separation," NASA TM X-62412.

Kussoy, M. I., and Horstman, C. C. (1989), "Documentation of Two- and Three-Dimensional Hypersonic Shock Wave/Turbulent Boundary Layer Interaction Flows," NASA TM 101075.

Kussoy, M. I., and Horstman, C. C. (1991), "Documentation of Two and Three-Dimensional Shock-Wave/Turbulent-Boundary-Layer Interaction Flows at Mach 8.2," NASA TM 103838.

Kussoy, M. I., Kim, K-S., and Horstman, C. C. (1991), "An Experimental Study of a Three-Dimensional Shock Wave/Turbulent Boundary-Layer Interaction at a Hypersonic Mach Number," AIAA Paper 91-1761, Honolulu, HI.

Kussoy, M. I., and Horstman, C. C. (1992), "Intersecting Shock-Wave/Turbulent Boundary-Layer Interactions at Mach 8.3," NASA TM 103909.

Kussoy, M. I., and Horstman, K. C. (1993), "Three-Dimensional Hypersonic Shock Wave/ Turbulent Boundary-Layer Interactions," *AIAA J.*, Vol. 31, No. 1, pp. 8-9.

Kussoy, M. I., Horstman, K. C., and Horstman, C. C. (1993), "Hypersonics Crossing Shock-Wave/Turbulent-Boundary-Layer Interactions," *AIAA J.*, Vol. 31, No. 12, pp. 2197-2203; also in AIAA Paper 93-0781, Reno, NV.

Jones, W.P., and Launder, B.E. (1972), "The Prediction of Laminarization with a Two Equation Model of Turbulence," *Int. J. of Heat and Mass Transfer*, Vol. 15, pp. 301-304.

Launder, B.E., and Sharma, B.I. (1974), "Application of the Energy-Dissipation Model of Turbulence to the Calculation of Flow Near a Spinning Disk," *Letters in Heat and Mass Transfer*, Vol. 1, pp. 131-138.

Lee, Y., Settles, G. S., and Horstman, C. C. (1992), "Heat Transfer Measurements and CFD Comparison of Swept Shock Wave/Boundary-Layer Interactions," AIAA Paper 92-3665, Nashville, TN.

Marvin, J. G. (1987), "Wind Tunnel Requirements for Computational Fluid Dynamics Code Verification," Paper 34, AGARD Symposium on Aerodynamic Data Accuracy and Quality, Requirements and Capabilities in Wind Tunnel Testing, Naples, Italy; also in NASA TM 100001.

Marvin, J. G. (1990), "Progress and Challenges in Modeling Turbulent Aerodynamic Flows," Engineering Turbulence Modeling and Experiments, editors W. Rodi and E. N. Genic, Elzevier, pp. 3-12; also in NASA TM 102811.

Marvin, J. G., and Coakley, T. J. (1990), "Turbulence Modeling for Hypersonic Flows," 2nd Joint Europe-US Short Course in Hypersonics, Air Force Academy, Colorado Springs, CO; also in NASA TM 101079, Jun. 1989, and 3d Joint US/Europe Short Course in Hypersonics, Aachen, W. Germany.

Marvin, J. G., Horstman, C. C., Lockman, W. K., and Strawa, A. W. (1991), "CFD Validation Experiments for NASP (U)," Tenth NASP Symp., Monterey, CA.

Marvin, J. G. (1992), "A CFD Validation Roadmap for Hypersonic Flows," AGARD 70th Fluid Dyn. Panel Meeting, Torino, Italy.

Marvin, J. G. (1992), "CFD Validation Experiments for Hypersonic Flows," AIAA Paper 92-4024, Nashville, TN.

Menter, F.R. (1993), "Zonal Two Equation k-ω Turbulence Models for Aerodynamic Flows," AIAA Paper 93-2906, Orlando, FL.

Narayanswami, N., Knight, D. D., Bogdonoff, S. M., and Horstman, C. C. (1991), "Crossing Shock Wave-Turbulent Boundary Layer Interactions," AIAA Paper 91-0649, Reno, NV.

Narayanswami, N., Knight, D. D., Bogdonoff, S. M., and Horstman, C. C. (1992), "Interaction Between Crossing Oblique Shocks and a Turbulent Boundary Layer," *AIAA J.*, Vol. 30, No. 8, pp. 1945-1952.

Narayanswami, N., Knight, D. D., and Horstman, C. C. (1992), "Investigation of a Hypersonic Crossing Shock Wave/Turbulent Boundary Layer Interaction Shock Waves," *AIAA J.*, Vol. 2, No. 4.

Narayanswami, Horstman, C. C., and Knight, D. D. (1993), "Computation of Crossing Shock/Turbulent Boundary Layer Interaction at Mach 8.3," AIAA Paper 93-0779, Reno, NV.

Prabhu, D. K., Tannehill, J. C., and Marvin, J. G. (1986), "Hypersonic Nonequilibrium Flow Fields over Wedges and Cones," NASP Tech. Symposium, Johns Hopkins Univ., Laurel, MD.

Prabhu, D. K., Tannehill, J. C., and Marvin, J. G. (1987), "A New PNS Code for Chemical Nonequilibrium Flows," AIAA Paper 87-0284, Reno, NV.

Prabhu, D. K., Tannehill, J. C., and Marvin, J. G. (1993), "A New PNS Code for Three-Dimensional Chemically Reacting Flows," AIAA 87-1472, Honolulu, HI.

Samimy, M., and Elliot, G.S. (1990), "Effects of Compressibility on the Characteristics of Free Shear Layers," *AIAA J.*, Vol. 28, No. 3, pp. 439-445.

Sarkar, S. (1991), "Modeling the Pressure-Dilatation Correlation," ICASE Report 91-42, NASA Langley Research Center.

Settles, G. S, and Dodson, L. J. (1991), "Hypersonic Shock/Boundary-Layer Interaction Database," NASA CR 177577.

Settles, G. S., and Dodson, L. J. (1993), "Hypersonic Turbulent Boundary-Layers and Free-Shear Layer Database," NASA CR 1776.

Settles, G. S, and Dodson, L. J. (1993), "Hypersonic Shock/Boundary-Layer Interaction Database: New and Corrected Data," Dept. of Mech. engrg., Penn State Univ., University Park, PA; also to be published as NASA CR.

Spaid, F. W., and Keener (1993), "Hypersonic Nozzle/After body CFD Code Validation Part 1: Experimental Measurements," AIAA Paper 93-0607, Reno, NV.

Viegas, J.R., and Rubesin, M.W. (1991), "A comparative Study of Several Compressibility Corrections to Turbulence Models Applied to High Speed Shear Layers," AIAA Paper 91-1783, Honolulu, HI.

Viegas, J.R., and Rubesin, M.W. (1992), "Assessment of Compressibility Corrections to the k-ε Model in High-Speed Shear Layers," *AIAA J.*, Vol. 30, No. 10, pp. 2369-2370.

Wilcox, D.C. (1991), "A Half Century Historical Review of the k-ω Model," AIAA Paper 91-0615, Reno, NV.

Wilcox, D.C. (1991), "Progress in Turbulence Modeling," AIAA Paper 91-1785, Honolulu, HI.

Zeman, O. (1990), "Dilatation Dissipation: The Concept and Application in Modeling Compressible Mixing Layers," *Physics of Fluids A*, Vol. 2.

Zhelotovodov, A. A., Borisov, A. V., Knight, D. D., Horstman, C. C., and Settles, G. S. (1992), "The Possibilities of Numerical Simulation of Shock Waves/Boundary Layer Interaction in Supersonic and Hypersonic Flows," Proceedings of International Conf. on the Methods of Aerophysical Research, pp. 164-170, Novosibirisk, Russia.

MILESTONES

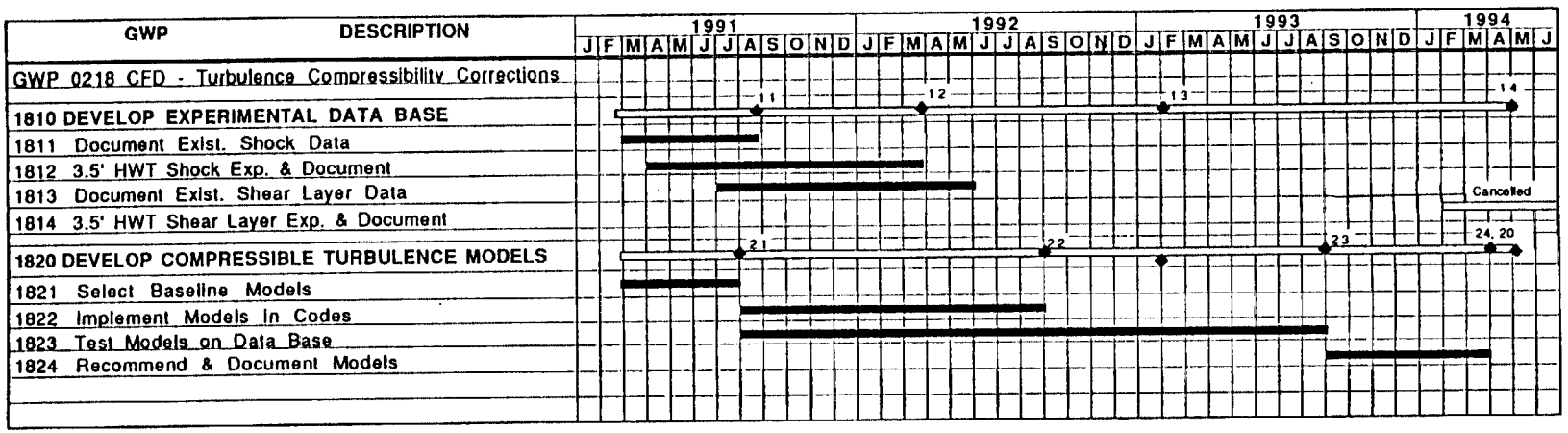

Fig. 1. Schedule of tasks and milestones of the research on GWP-18.

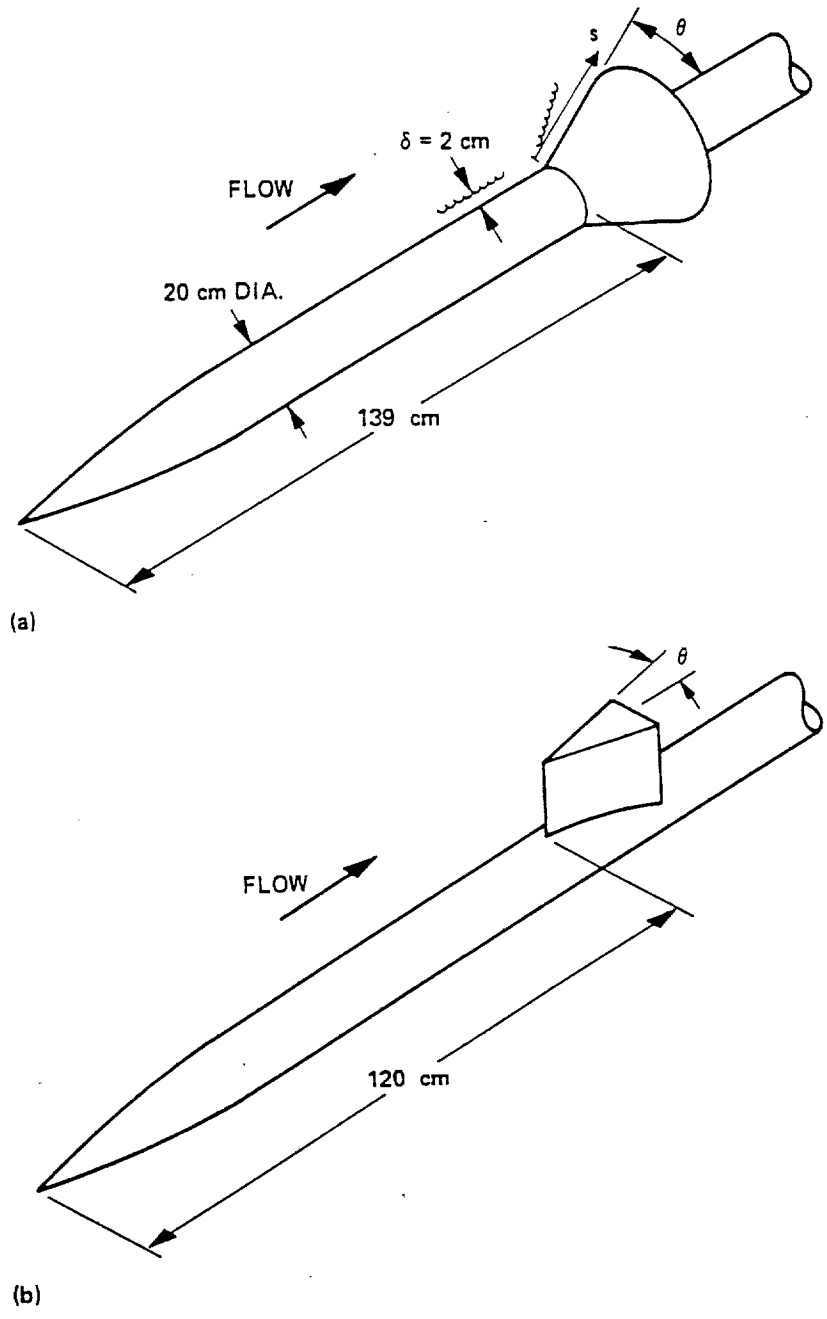

Fig. 2. Ogive-cylinder experimental configuration with (a) flare attached and (b) with fin attached of Kussoy and Horstman (1989).

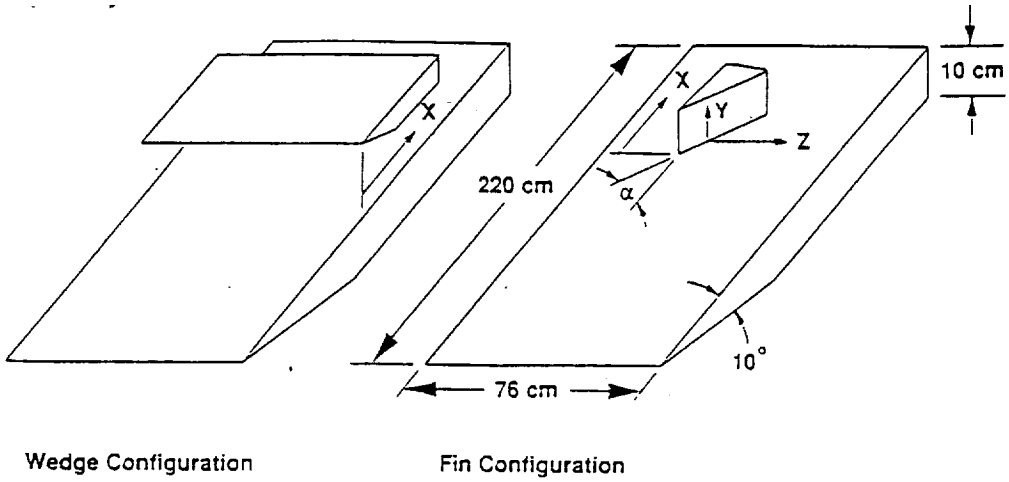

Fig. 3. 2-D wedge and 3-D vertical fin on flat plate configuration of Kussoy and Horstman (1991a)

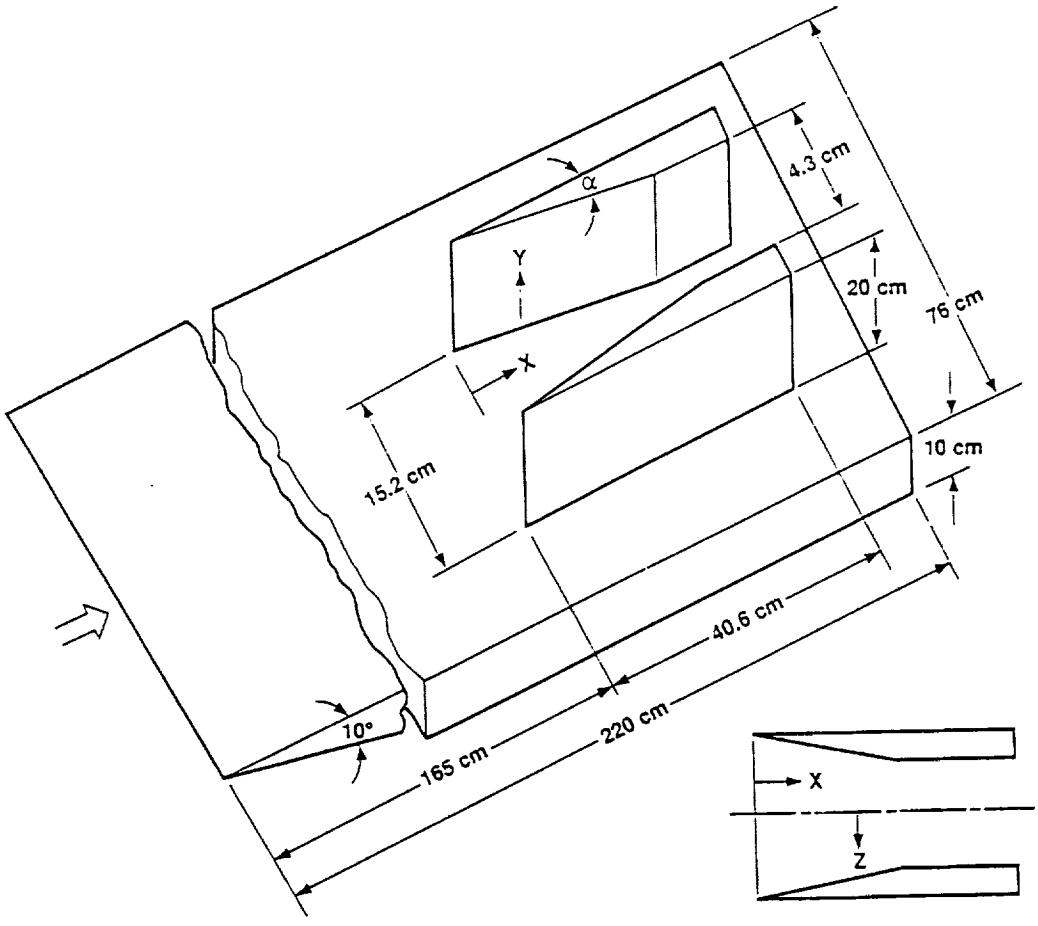

Fig. 4. Crossing shocks generated with two vertical fins on flat plate configuration of Kussoy and Horstman (1992).

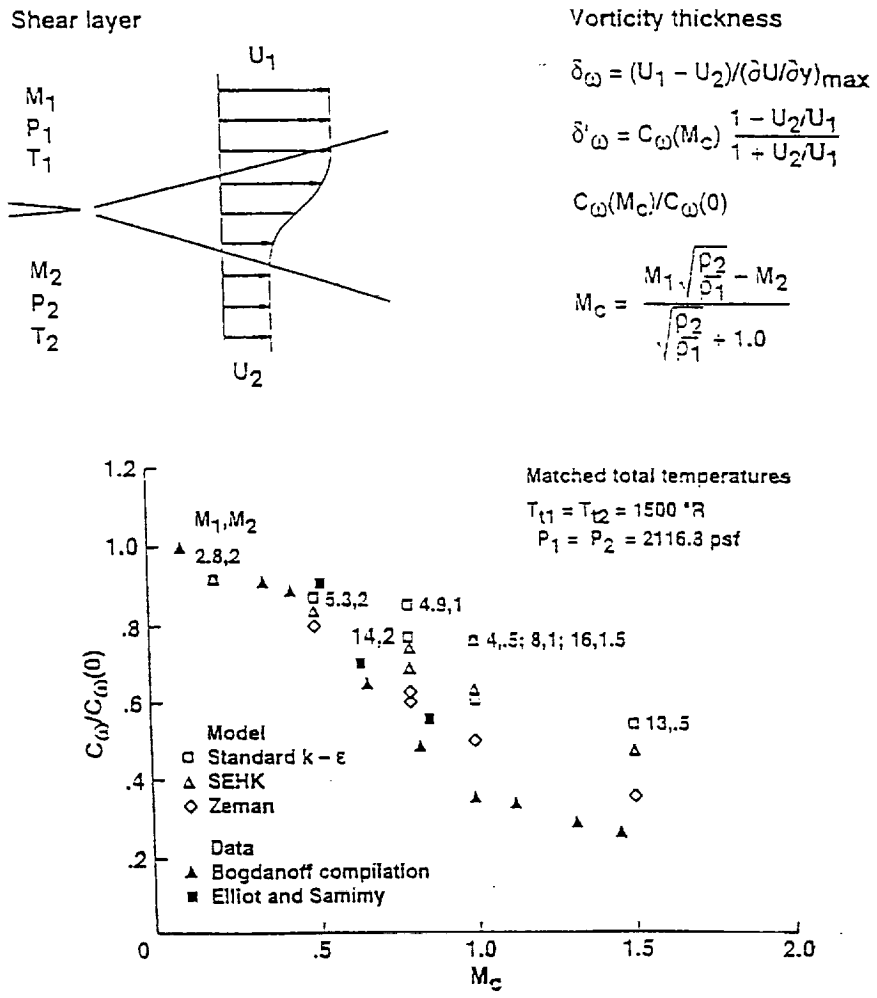

Fig. 5. Effect of compressibility on normalized vorticity thickness growth rate for mixing layer (Viegas and Rubesin (1991, 1992)).

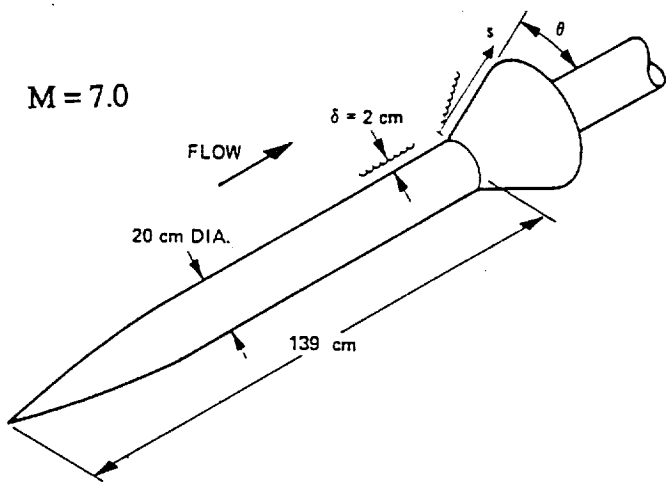

Fig. 6a. Axisymmetric compression generated with ogive-cylinder-flare configuration of Kussoy and Horstman (1989).

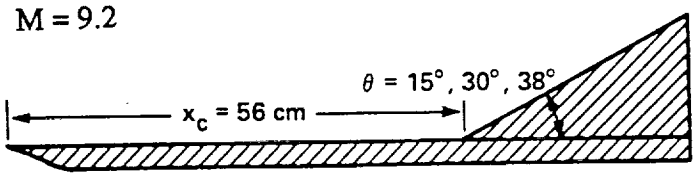

Fig. 6b. 2-D planar compression ramp configuration of Coleman and Stollery (1972).

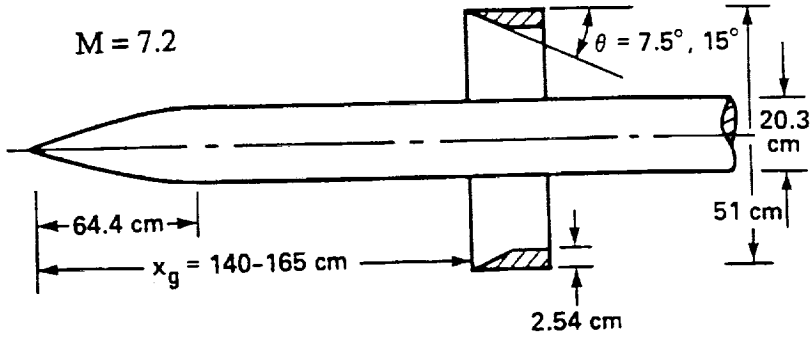

Fig. 6c. Axisymmetric impinging shock generated with a cone-ogive cylinder and an annular fin configuration of Kussoy and Horstman (1975).

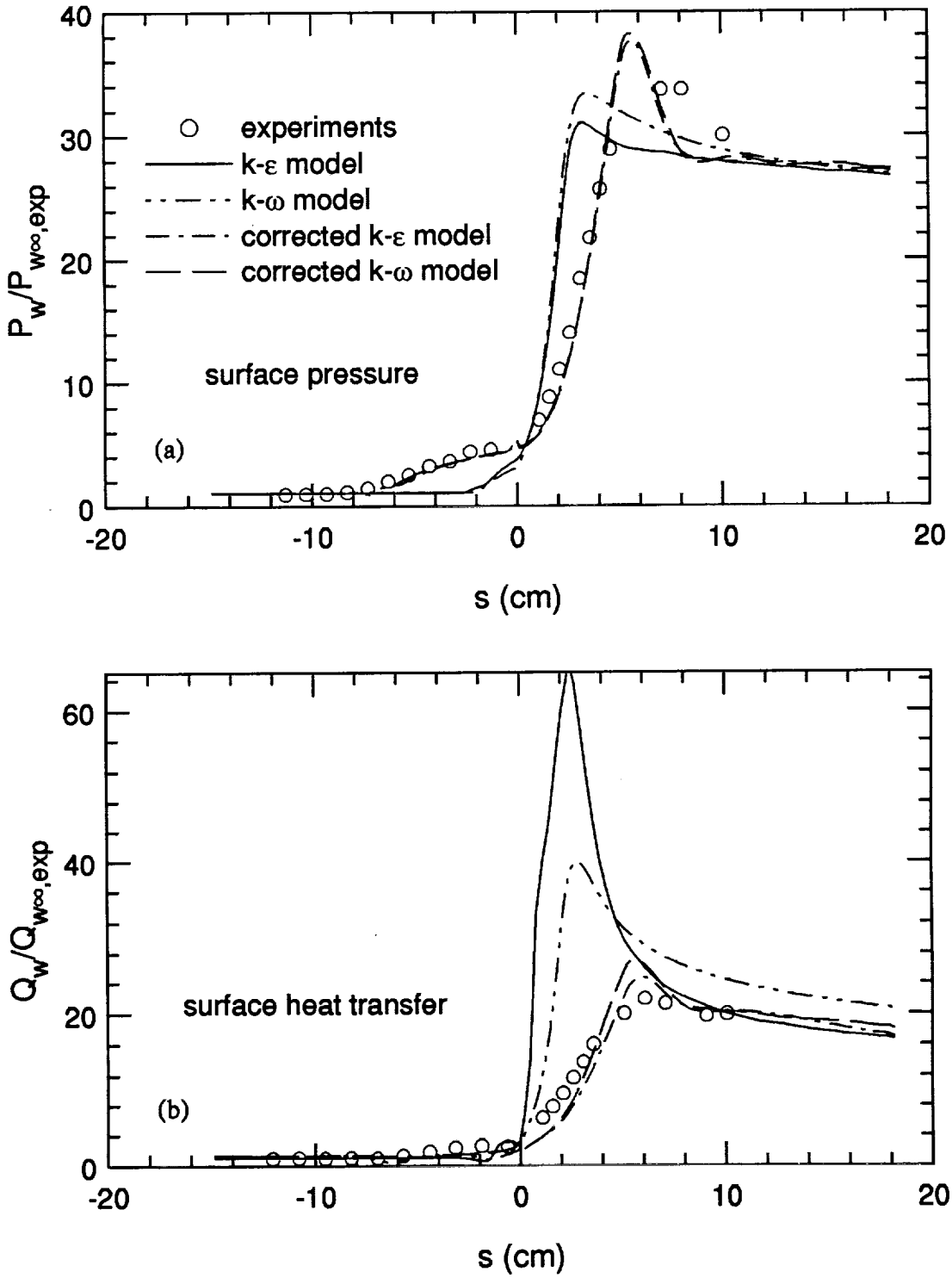

Fig. 7. Surface pressure (a) and heat transfer (b) in axisymmetric compression flow of Kussoy and Horstman (1989), geometry shown in Fig. 6a.

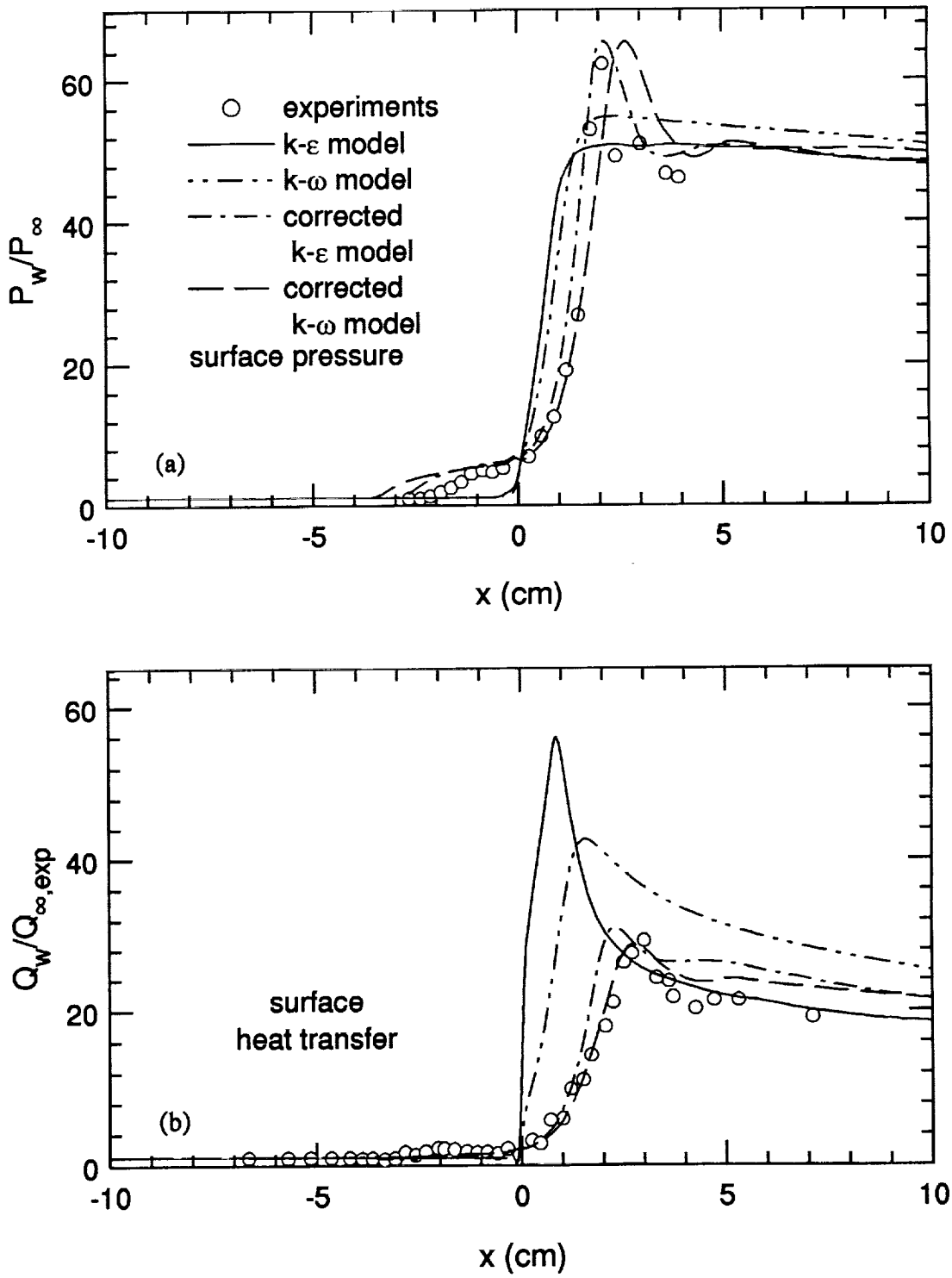

Fig. 8. Surface pressure (a) and heat transfer (b) in 2-D planar compression ramp flow of Coleman and Stollery (1972), geometry shown in Fig 6b.

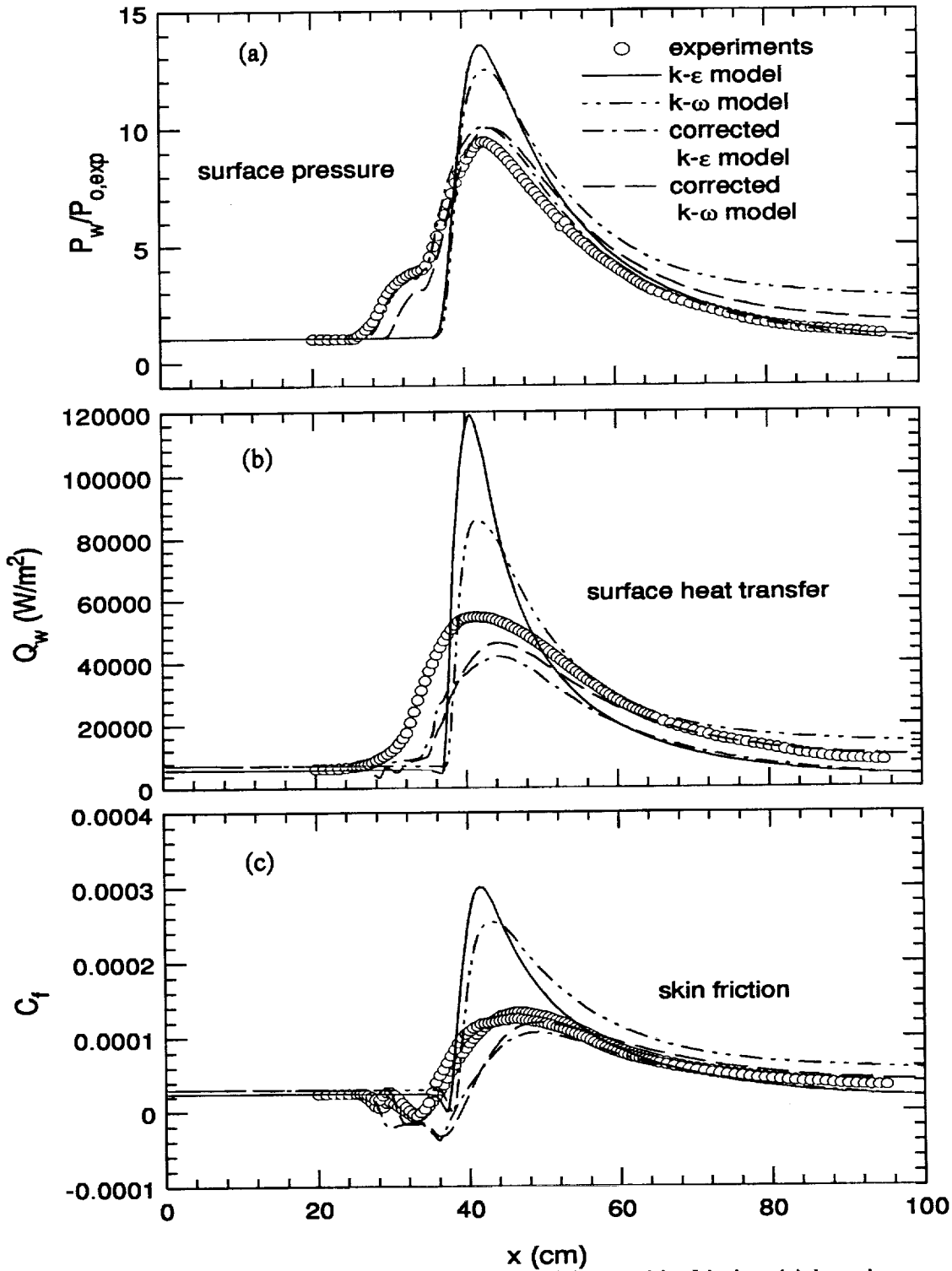

Fig. 9. Surface pressure (a), heat transfer (b) and skin friction (c) in axisymmetric impinging shock flow of Kussoy and Horstman (1975), geometry shown in Fig 6c.

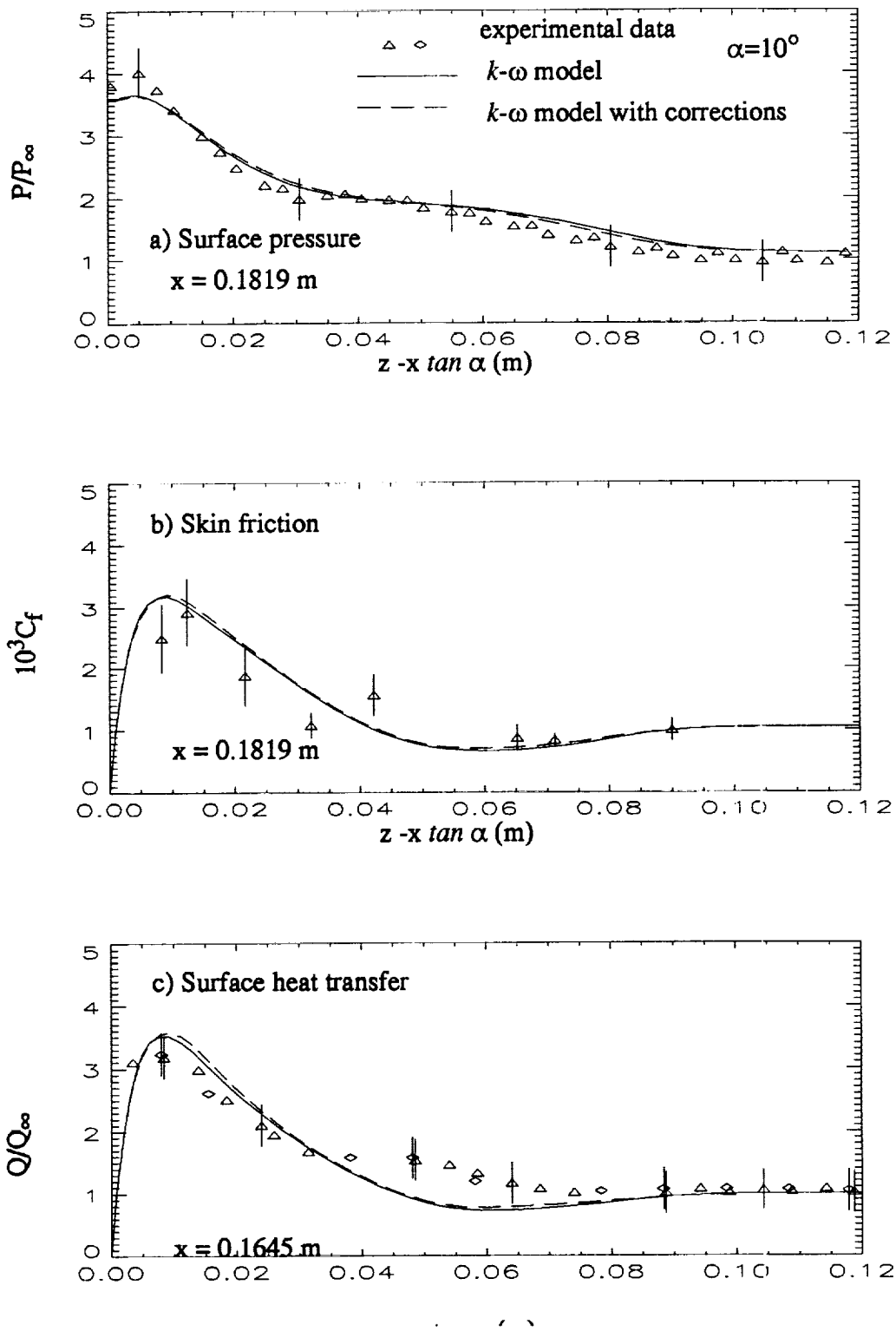

Fig. 10. Surface flow predictions in the 3-D vertical fin interaction flow (α=10° case) of Kussoy and Horstman (1991a), geometry shown in Fig. 3.

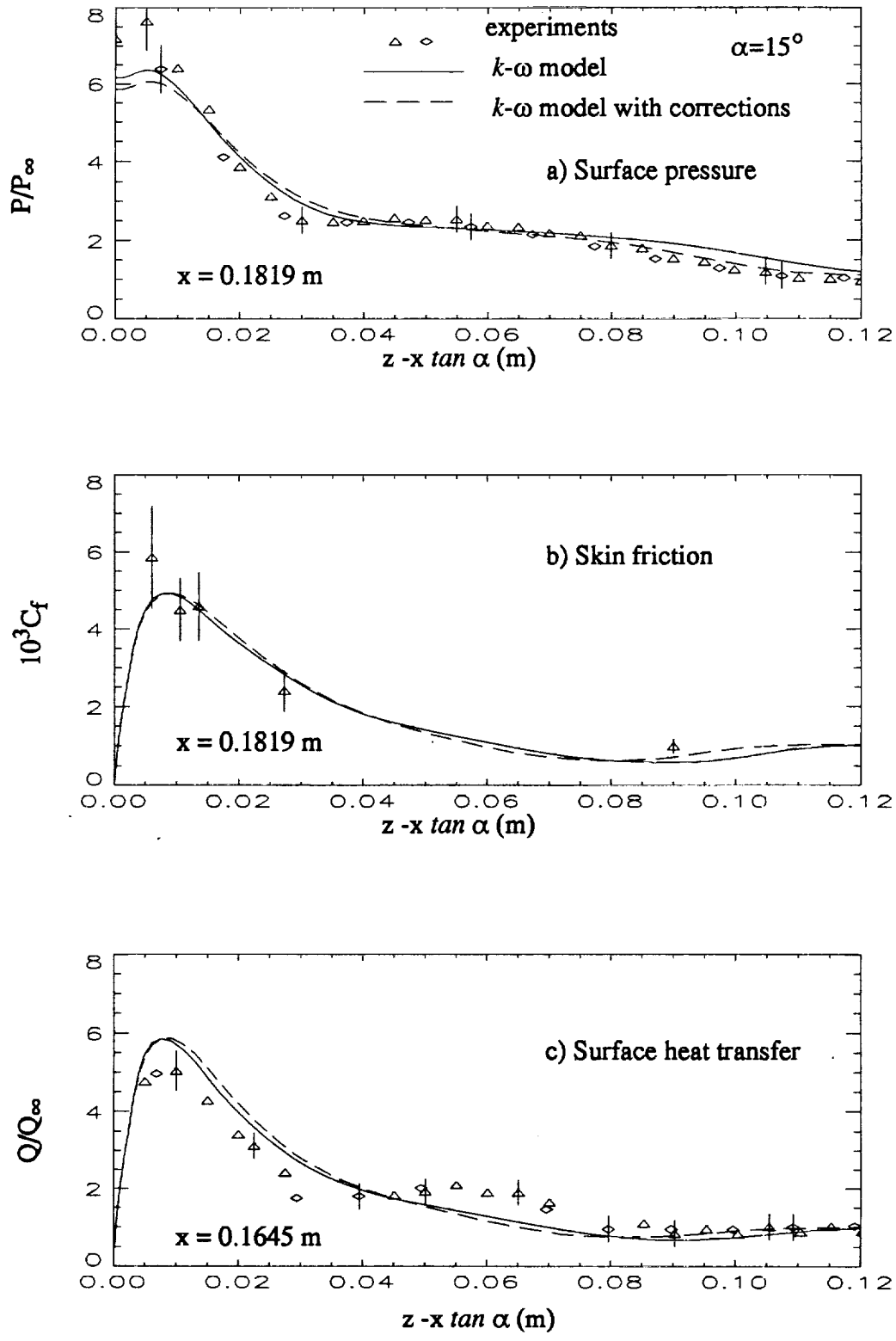

Fig. 11. Surface flow predictions in the 3-D vertical fin interaction flow (α=15° case) of Kussoy and Horstman (1991a), geometry shown in Fig. 3.

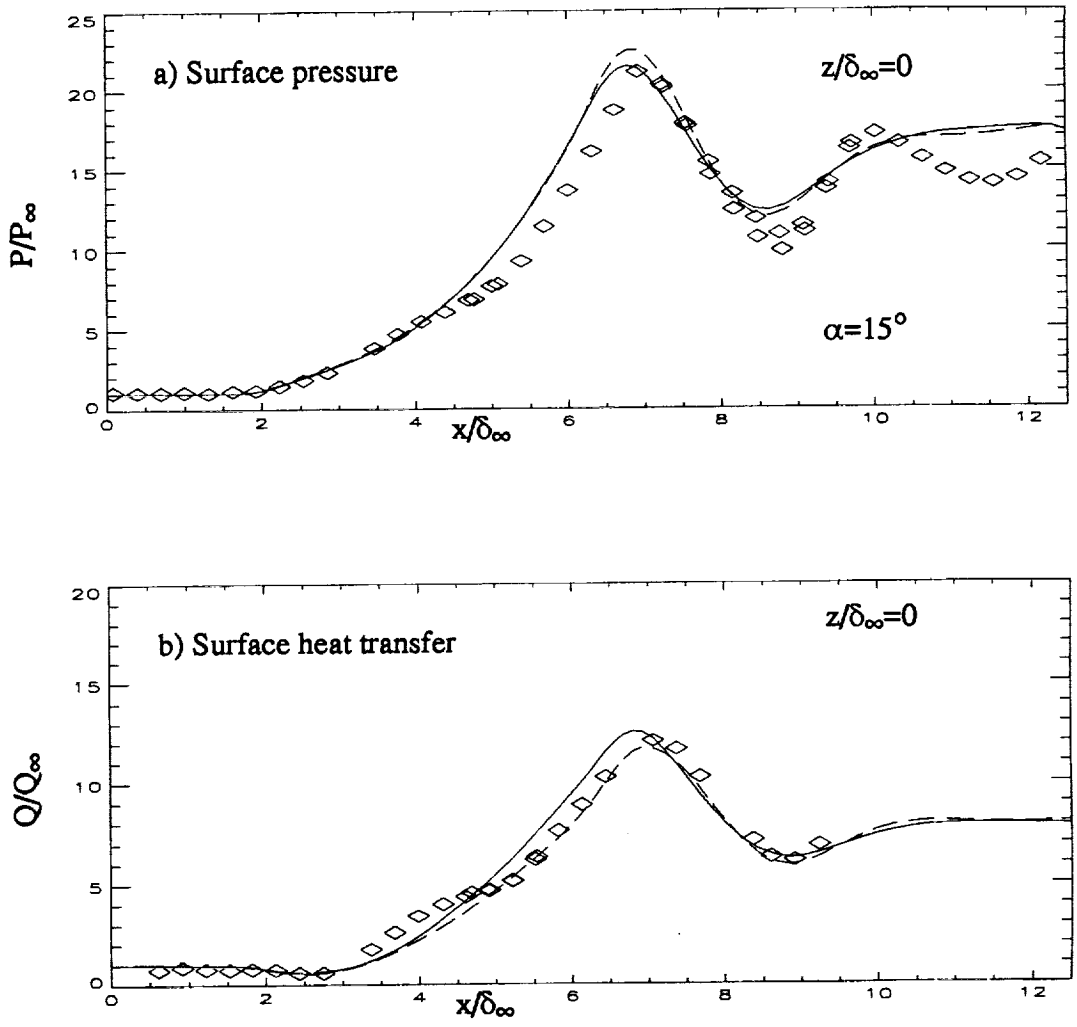

Fig. 12. Surface flow predictions in the symmetry plane of the 3-D crossing shock flow (α=15° case) of Kussoy and Horstman (1992), geometry shown in Fig. 4. (Symbols represent experimental data, — k-ω model, and --- k-ω model with corrections).

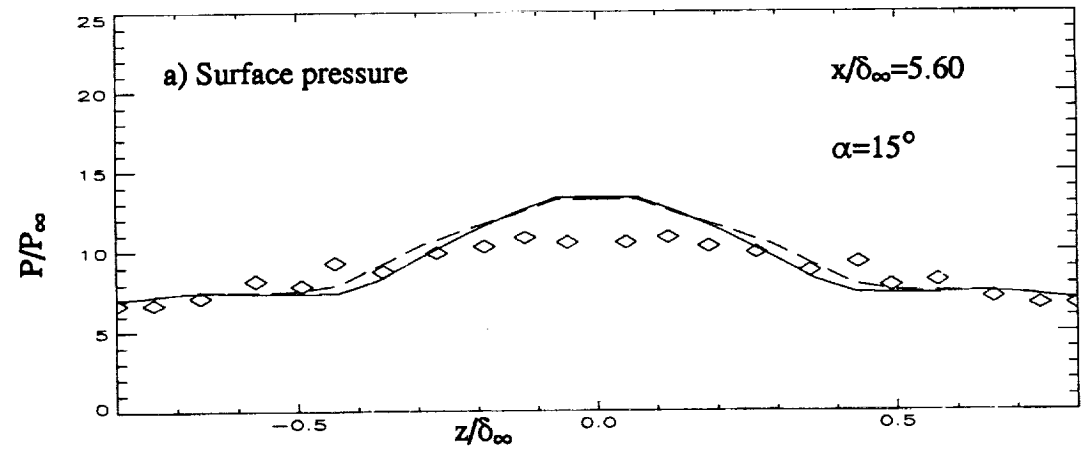

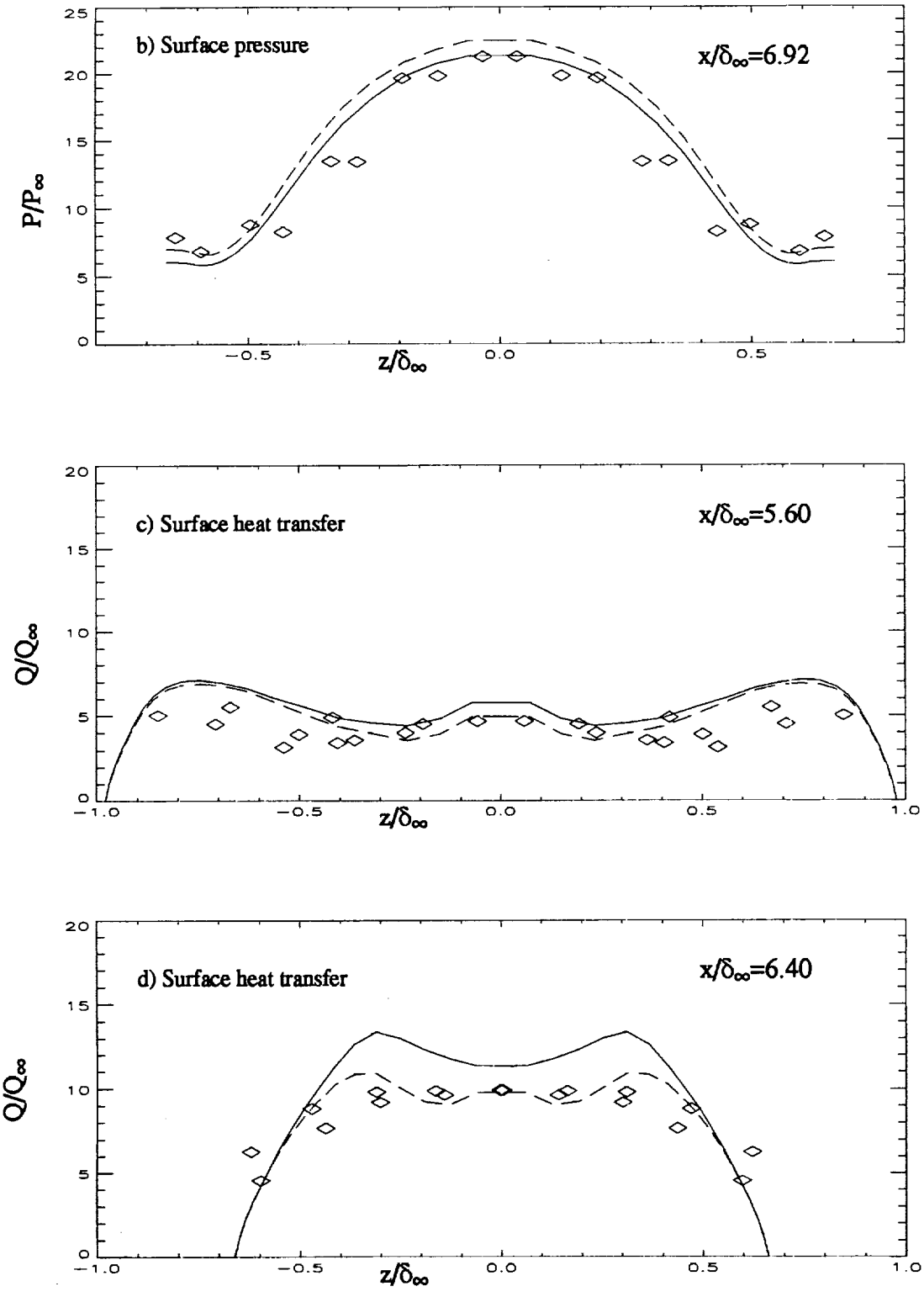

Fig. 13. Surface flow quantities in the 3-D crossing shock interaction flow (α=15° case) of Kussoy and Horstman (1992), geometry shown in Fig. 4. (Symbols represent experimental data, — k-ω model, and --- k-ω model with corrections).

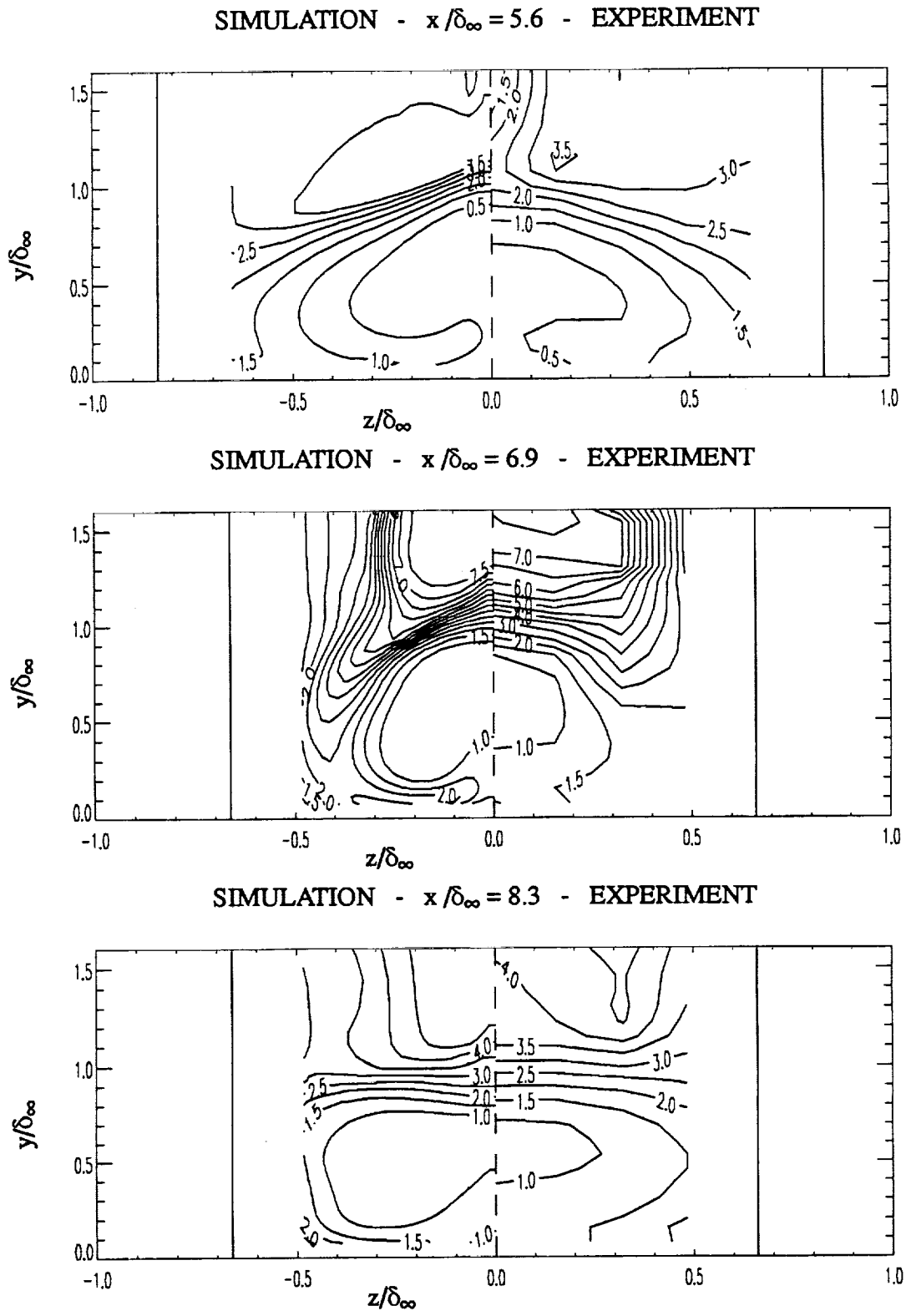

Fig. 14. Pitot pressure contours on cross-sections of 3-D crossing shock interaction flow (α=15° case) of Kussoy and Horstman (1992), geometry shown in Fig. 4. (The fin leading edges are located at $x = 0$, and δ_∞ is the thickness of the undisturbed turbulent boundary layer at $x = 0$).

REPORT DOCUMENTATION PAGE

Form Approved
OMB No. 0704-0188

1. AGENCY USE ONLY *(Leave blank)*	2. REPORT DATE	3. REPORT TYPE AND DATES COVERED
	May 1994	Technical Memorandum

4. TITLE AND SUBTITLE

Turbulence Compressibility Corrections

5. FUNDING NUMBERS

505-70-59

6. AUTHOR(S)

T. J. Coakley, C. C. Horstman, J. G. Marvin, J. R. Viegas, J. E. Bardina, P. G. Huang, and M. I. Kussoy

7. PERFORMING ORGANIZATION NAME(S) AND ADDRESS(ES)

Ames Research Center
Moffett Field, CA 94035-1000

8. PERFORMING ORGANIZATION REPORT NUMBER

A-94091

9. SPONSORING/MONITORING AGENCY NAME(S) AND ADDRESS(ES)

National Aeronautics and Space Administration
Washington, DC 20546-0001

10. SPONSORING/MONITORING AGENCY REPORT NUMBER

NASA TM-108827

11. SUPPLEMENTARY NOTES

Point of Contact: T. J. Coakley, Ames Research Center, MS 229-1, Moffett Field, CA 94035-1000; (415) 604-6451

12a. DISTRIBUTION/AVAILABILITY STATEMENT

Unclassified — Unlimited
Subject Category 34

12b. DISTRIBUTION CODE

13. ABSTRACT ***(Maximum 200 words)***

The basic objective of this research was to identify, develop and recommend turbulence models which could be incorporated into CFD codes used in the design of the National AeroSpace Plane vehicles. To accomplish this goal, a combined effort consisting of experimental and theoretical phases was undertaken. The experimental phase consisted of a literature survey to collect and assess a database of well documented experimental flows, with emphasis on high-speed or hypersonic flows, which could be used to validate turbulence models. Since it was anticipated that this database would be incomplete and would need supplementing, additional experiments in the NASA Ames 3.5-Foot Hypersonic Wind Tunnel (HWT) were also undertaken. The theoretical phase consisted of identifying promising turbulence models through applications to simple flows, and then investigating more promising models in applications to complex flows. The complex flows were selected from the database developed in the first phase of the study. For these flows it was anticipated that model performance would not be entirely satisfactory, so that model improvements or corrections would be required. The primary goals of the investigation were essentially achieved. A large database of flows was collected and assessed, a number of additional hypersonic experiments were conducted in the Ames HWT, and two turbulence models (κ–ε and κ–ω models with corrections) were determined which gave superior performance for most of the flows studied and are now recommended for NASP applications.

14. SUBJECT TERMS

Hypersonic, Turbulence, Modeling

15. NUMBER OF PAGES

40

16. PRICE CODE

A03

17. SECURITY CLASSIFICATION OF REPORT	18. SECURITY CLASSIFICATION OF THIS PAGE	19. SECURITY CLASSIFICATION OF ABSTRACT	20. LIMITATION OF ABSTRACT
Unclassified	Unclassified		